



A mesoporous $\text{TiO}_{2-x}\text{N}_x$ photocatalyst prepared by sonication pretreatment and in situ pyrolysis

Guisheng Li^a, Jimmy C. Yu^{a,*}, Dieqing Zhang^a, Xianluo Hu^a, Woon Ming Lau^b

^a Department of Chemistry and Environmental Science Programme, The Chinese University of Hong Kong, Shatin, New Territories, Hong Kong, China

^b Surface Science Western, University of Western Ontario, London, Ontario N6A 5B7, Canada

ARTICLE INFO

Keywords:

Titanium dioxide
Nitrogen doping
Pyrolysis
Chelation
Sonication

ABSTRACT

A novel method for preparing a visible-light-driven mesoporous $\text{TiO}_{2-x}\text{N}_x$ photocatalyst has been developed. It involves the in situ pyrolysis of the product from a chelation reaction under sonication between TiCl_4 and ethylenediamine in an ethanol solution of the triblock copolymer F127. The as-prepared photocatalysts exhibit very strong photoactivity in the photocatalytic oxidation of methylene blue under irradiation in the visible spectral region. The samples were characterized by spectroscopic techniques including ultraviolet–visible light reflectance (UV–vis), X-ray photoelectron spectroscopy (XPS), electron spin resonance (ESR), X-ray diffraction (XRD), scanning electron microscopy (SEM), and transmission electron microscopy (TEM). The effects of ultrasound on the physicochemical properties and photoactivity of mesoporous $\text{TiO}_{2-x}\text{N}_x$ are discussed based on the characterization results.

© 2009 Elsevier B.V. All rights reserved.

1. Introduction

The application of TiO_2 photocatalyst for degradation of various kinds of organic and inorganic pollutants has been extensively studied [1]. A major limitation of TiO_2 is that with a band gap of 3.2 eV it can only be activated by UV radiation [2]. A great deal of effort has been made to develop the visible-light-responsive materials by narrowing the band gap of TiO_2 . These include substituting the lattice Ti ion with various kinds of transition-metal ions [3,4] and doping of TiO_2 with impurities such as carbon, nitrogen, fluorine, or sulfur [5–10]. Surface area and crystallinity are important factors that affect the activity of a photocatalyst. A highly crystalline mesoporous TiO_2 with a large surface area is obviously advantageous [11,12]. Surprisingly, reports on the preparation of N-doped mesoporous TiO_2 are scarce. Non-mesoporous N-doped TiO_2 materials are usually prepared by treating TiO_2 under NH_3 atmosphere at very high temperatures, such as 500 °C. Such an approach is energy intensive and the resulting products tend to have low surface area owing to agglomeration. We have developed recently a method to fabricate mesoporous $\text{TiO}_{2-x}\text{N}_x$ through thermal treatment of NH_3 -adsorbed TiO_2 hydrosol gels. The undesirable crystal growth during calcination was effectively inhibited by the addition of ZrO_2 as a structure stabilizer [13]. Herein, we describe a novel route to N-doped mesoporous TiO_2 without adding any stabilizers. This is done by in situ pyrolysis of the product of a chelation reac-

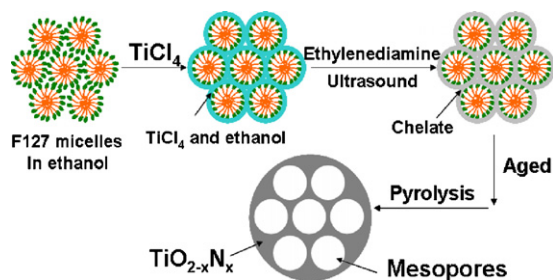
tion between TiCl_4 and ethylenediamine in an ethanol solution of surfactant under ultrasound irradiation. The use of ultrasound to enhance the rate of reaction has become a routine synthetic technique for many homogenous and heterogeneous chemical systems [14,15]. Sonochemistry has been used to prepare various oxides and amorphous metal powders [15–17]. In the present work, ultrasonic irradiation can help disperse the TiO_2 particles, increase the surface area, enlarge the pore volume, and incorporate a relatively high concentration of nitrogen into the TiO_2 framework.

2. Experimental

2.1. Catalyst preparation

To synthesize mesoporous $\text{TiO}_{2-x}\text{N}_x$, we used titanium tetrachloride (Aldrich) as a titanium source, a triblock copolymer F127 ($\text{EO}_{106}\text{PO}_{70}\text{EO}_{106}$, Aldrich) as a structure direction agent, and ethylenediamine as a source of nitrogen. In a typical synthesis, an amount of 1.84 g of F127 was dissolved in 60 ml ethanol (EtOH). To this clear solution, 0.0125 mol TiCl_4 was added dropwise with vigorous stirring at room temperature. The product was labeled Solution A. A second solution was prepared by mixing 5.2 ml ethylenediamine with 20 ml ethanol. This mixture was added dropwise to Solution A under sonication for 1 h in an ultrasonic cleaning bath (Branson ultrasonic cleaner, model 3210E DTH, 47 kHz, 120 W, USA). The reaction mixture was aged for 24 h in a closed autoclave at 180 °C to form mono-dispersed $\text{TiO}_{2-x}\text{N}_x$ precursor particles. The particles were filtered and dried at 100 °C in air in order to vaporize the residual alcohol, and then calcined at 350 °C or 450 °C

* Corresponding author. Tel.: +852 2609 6268; fax: +852 2603 5057.
E-mail address: jimyu@cuhk.edu.hk (J.C. Yu).



Scheme 1. The synthesis route to mesoporous $\text{TiO}_{2-x}\text{N}_x$.

in air for 12 h or 4 h, respectively to obtain mesoporous $\text{TiO}_{2-x}\text{N}_x$ photocatalysts. A graphical illustration for the synthesis route is shown in **Scheme 1**. When the concentration is higher than the critical micellar concentration, the surfactant micellar structure can form liquid-crystalline mesophase through self-assembly. Such liquid-crystalline mesophase can be used to prepare mesoporous inorganic materials [18]. TiCl_4 and surfactant can co-assemble and form nanocomposites containing ordered surfactant lyotropic liquid-crystalline phases. Under sonication, the chelation of Ti^{4+} ions by ethylenediamine formed the metal complex surrounding the micellar structure. Finally, through the pyrolysis of the chelate and surfactant composite, $\text{TiO}_{2-x}\text{N}_x$ with a mesoporous structure is obtained. The FT-IR spectra in **Fig. 1** confirm almost complete removal of the surfactant at a temperature of 350°C . For simplicity, the mesoporous $\text{TiO}_{2-x}\text{N}_x$ samples prepared with and without ultrasonic irradiation are abbreviated MU- $\text{TiO}_{2-x}\text{N}_x$ and M- $\text{TiO}_{2-x}\text{N}_x$.

2.2. Catalyst characterization

Wide-angle X-ray diffraction measurements were carried out using a Bruker D8 Advance X-ray diffractometer with $\text{Cu K}\alpha$ radiation. The N_2 -sorption isotherms were recorded at 77 K using a Micromeritics ASAP 2010 instrument. The Brunauer–Emmett–Teller approach was used for the determination of the surface area. X-ray photoelectron spectroscopy was performed with a VG scientific ESCA Lab Mark II spectrometer. All binding energy (BE) values were calibrated by using the standard BE value of contamination carbon ($\text{C}_{1\text{S}} = 284.6\text{ eV}$) as a reference. Standard transmission electron microscopy images were recorded using a CM-120 microscope (Philips, 120 kV). The morphology of the samples was examined by a LEO 1450 VP scanning micro-

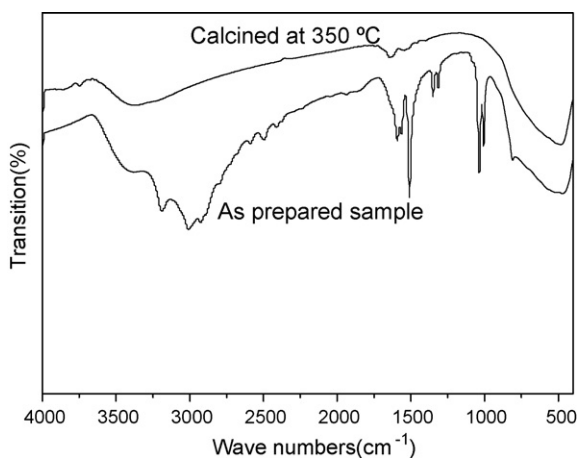


Fig. 1. FT-IR spectra of the $\text{TiO}_{2-x}\text{N}_x$ sample before (as-prepared $\text{TiO}_{2-x}\text{N}_x$) and after heat treatment (calcined at 350°C).

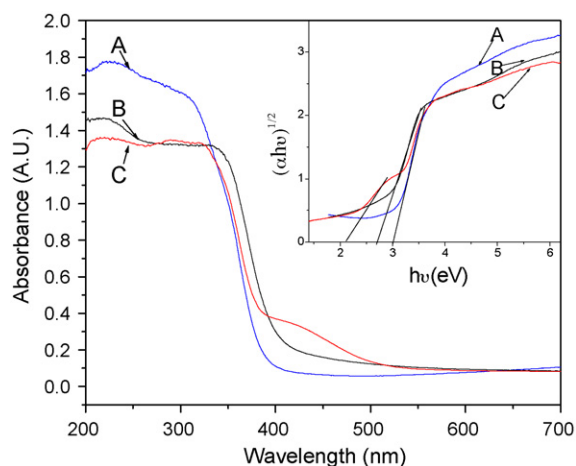


Fig. 2. UV-visible absorption spectra of (A) pure TiO_2 (P25), (B) M- $\text{TiO}_{2-x}\text{N}_x$ annealed at 350°C and (C) MU- $\text{TiO}_{2-x}\text{N}_x$ annealed at 350°C . Inset: plots of $(\alpha h\nu)^{1/2}$ versus photon energy ($h\nu$) for the above samples.

scope. FT-IR spectra on pellets of the samples mixed with KBr were recorded on a Nicolet Magna 560 FT-IR spectrometer at a resolution of 4 cm^{-1} . The reflectance spectra of the samples over a range of 200–800 nm were recorded by the Varian Cary 100 Scan UV-vis system (USA) equipped with a Labsphere diffuse reflectance accessory (USA). Electron spin resonance (ESR) spectra were obtained using a Bruker model ESP 300E ESR spectrometer. The settings for the ESR spectrometer were center field 3480.00 G, microwave frequency 9.79 GHz, and power 5.05 mW.

2.3. Photocatalytic activity test

The photocatalytic oxidation of methylene blue was carried out in an aqueous solution at ambient temperature. Briefly, in a 100 ml beaker, 0.08 g mesoporous $\text{TiO}_{2-x}\text{N}_x$ was mixed with 60 ml aqueous solution containing 10 ppm methylene blue. The mixture was stirred for 1 h until reaching adsorption equilibrium. The photocatalytic oxidation of methylene blue was initiated by irradiating the reaction mixture with a commercial 300 W tungsten halogen spotlight surrounded with a filter that restricted the illumination to the 400–660 nm range [19,20]. At 1-h time intervals, 1 mL of the solution was pipetted into a cuvette for measuring the absorbance at 660 nm with a Varian Cary 100 Scan UV-vis system (USA).

3. Results and discussion

3.1. UV-vis spectroscopy

The UV-visible absorption spectra of the mesoporous $\text{TiO}_{2-x}\text{N}_x$ samples are shown in **Fig. 2**. The inset in **Fig. 2** shows the optical absorption edge (in eV). The optical band edge of the mesoporous $\text{TiO}_{2-x}\text{N}_x$ exhibits a marked red shift with respect to that of pure TiO_2 (3.1 eV). The band gap of the sample prepared with ultrasound pretreatment is 2.2 eV which is lower than the 2.6 eV for the sample obtained without sonication. This difference of 0.4 eV is due to the different amount of nitrogen doped into the TiO_2 framework as shown in the XPS results.

3.2. X-ray photoelectron spectroscopy (XPS)

XPS profiles of the mesoporous $\text{TiO}_{2-x}\text{N}_x$ samples are shown in **Fig. 3**. The mesoporous $\text{TiO}_{2-x}\text{N}_x$ sample prepared with sonication has a nitrogen content of 4.1% in weight. This is much higher than the 1.9% in the sample obtained without ultrasonic treatment. How-

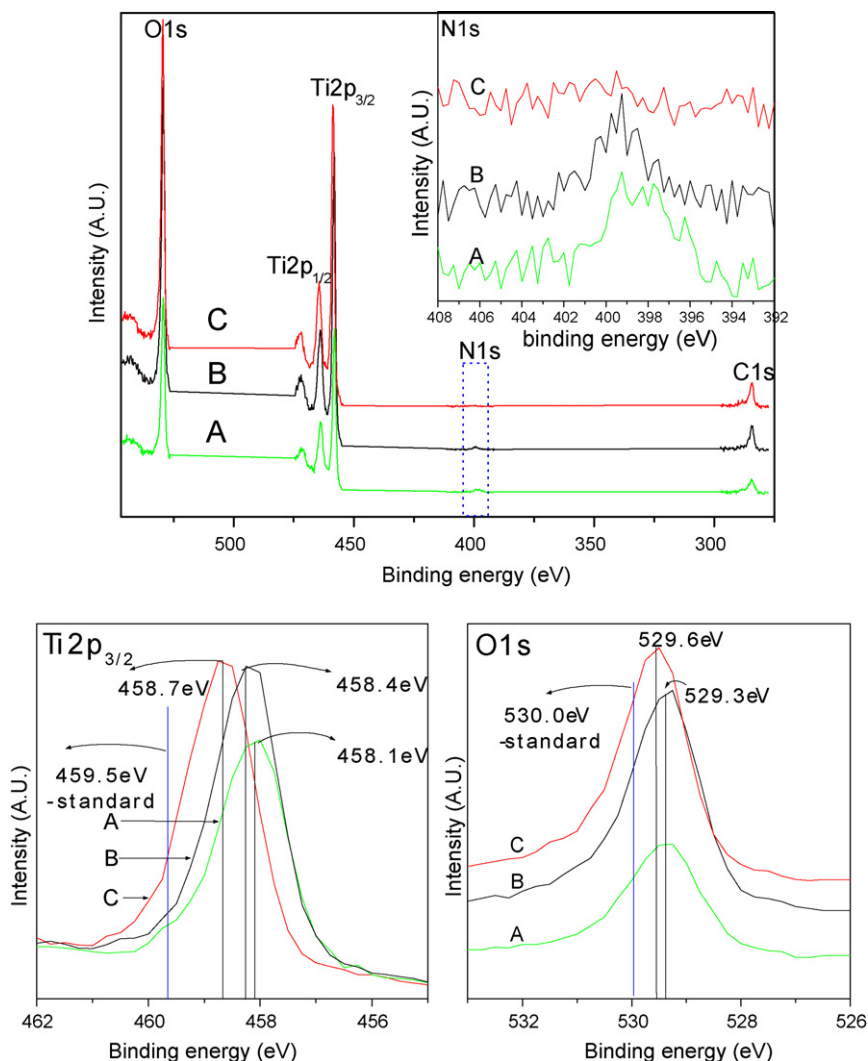


Fig. 3. X-ray photoelectron spectra of (A) MU-TiO_{2-x}N_x annealed at 350 °C, (B) M-TiO_{2-x}N_x annealed at 350 °C and (C) MU-TiO_{2-x}N_x annealed at 450 °C.

ever, when the calcination temperature was increased to 450 °C, the nitrogen content decreased from 4.1% to 1.1%. In order to prevent the loss of doped nitrogen, the calcination temperature should be kept as low as possible. In this work, 350 °C was chosen as the optimum calcination temperature. Fine anatase crystalline was obtained (see XRD results). For all of the samples, the BE value of N 1s is about 398.6 eV. It is derived from the presence of O–Ti–N linkages in the crystalline TiO₂ lattice [21]. It is interesting that the binding energy of Ti 2p_{3/2} can be further decreased through introducing higher nitrogen content to the TiO_{2-x}N_x samples. These BE values are much lower than the standard BE value of 459.5 eV for the pure TiO₂. The negative shift of binding energy of Ti 2p_{3/2} is due to the conversion of Ti⁴⁺ to Ti³⁺ caused by the substitution of nitrogen for oxygen [22]. As for the O 1s level, the peaks corresponding to the oxygen in the mesoporous TiO_{2-x}N_x samples shifted negatively by 0.4–0.7 eV in comparison with the pure TiO₂. These results further confirm the formation of O–Ti–N, in which electrons transferred from the N to the Ti and the O atoms due to the higher electronegativity of oxygen than that of nitrogen, making N electron-deficient while both the Ti and O electron-enriched [23].

3.3. Electron microscopy

As shown in the SEM images (Fig. 4A and B), the samples are mainly composed of 1–2 μm spherical particles. For the M-TiO_{2-x}N_x

sample, most particles are aggregated together into monolith blocks. However, the sample obtained through ultrasonic irradiation is uniform and well dispersed. A larger surface area is present for the adsorption of reactant molecules and more active sites are available for the photocatalytic reaction. Fig. 4C and D are the TEM images. The mesoporous structures are well defined, but the mesophases are of the short-range order. This is probably related to the crystallization of the channel walls, which destroys the long-range order mesoporous structure [24]. The selected-area electron diffraction patterns (insets of Fig. 4C and D) and the HRTEM image in Fig. 4E clearly reveal the anatase nanocrystalline nature in the pore walls of the samples. The wide-angle XRD results (Fig. 5) further confirm the existence of well-defined anatase nanocrystals in the samples. Such high anatase crystallinity of the mesoporous TiO₂ greatly enhances the activity of the oxidation of organic compounds because it effectively inhibits the recombination of photogenerated electrons and holes [25,26].

3.4. BET analysis

Fig. 6 shows the N₂ adsorption/desorption isotherms of the mesoporous TiO_{2-x}N_x samples. Results obtained from the Barrett–Joyner–Halenda (BJH) analysis of pore size distribution are shown in the inset. A clear hysteresis loop at high relative pressure of about 0.4–0.8 is observed, which is related to the capillary

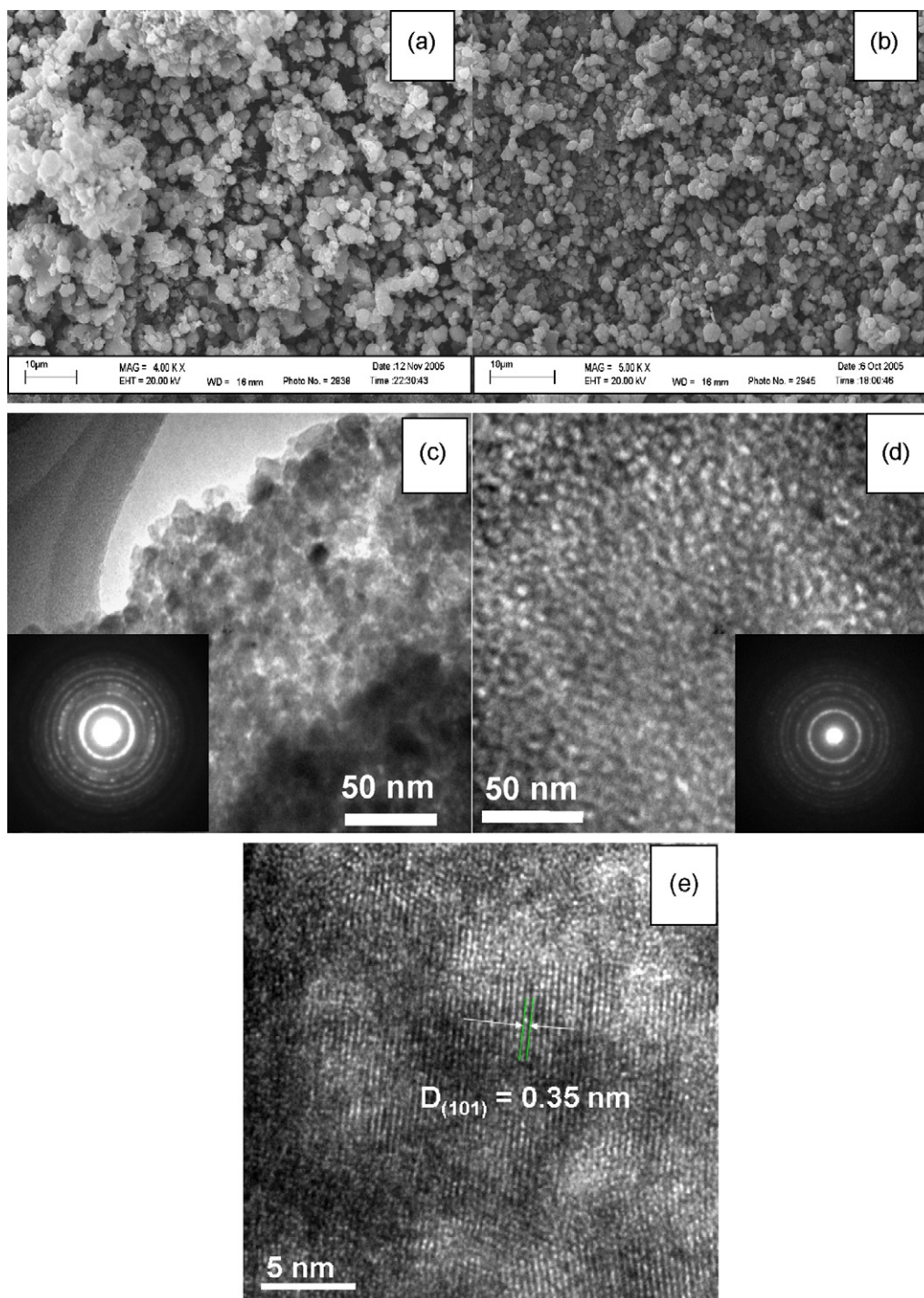


Fig. 4. SEM and TEM figures of (A and C) M-TiO_{2-x}N_x annealed at 350 °C; (B and D) MU-TiO_{2-x}N_x annealed at 350 °C; and (E) HRTEM of (D).

Table 1
Synthesis conditions and physicochemical properties of the mesoporous TiO_{2-x}N_x samples.

Sample	Sonication	Calcination temperature (°C)	S _{BET} ^a (m ² g)	Pore diameter ^b (nm)	Pore volume ^c (cm ³ g)
A	Yes	350	180.2	6.7	0.27
B	Yes	450	143.5	7.8	0.28
C	No	350	122.7	3.4	0.14

^a BET surface area calculated from the linear part of the BET plot ($P/P_0 = 0.1-0.2$).

^b Average pore diameter estimated using the desorption branch.

^c Total pore volume taken from the volume of N₂ adsorbed at $P/P_0 = 0.995$.

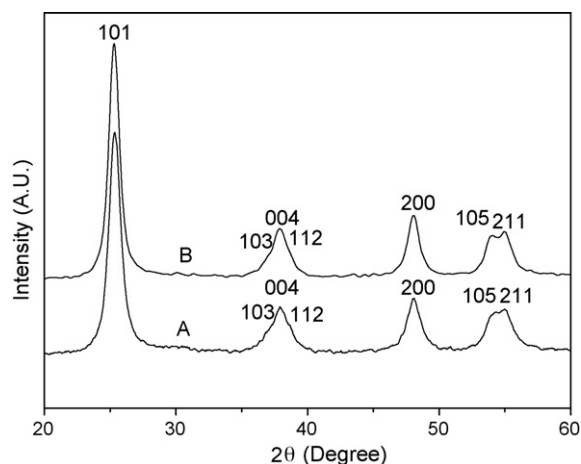


Fig. 5. XRD patterns in high (20–60°) and low (0.8–5°) angle regions for (A) MU-TiO_{2-x}N_x calcined at 350 °C and (B) M-TiO_{2-x}N_x calcined at 350 °C.

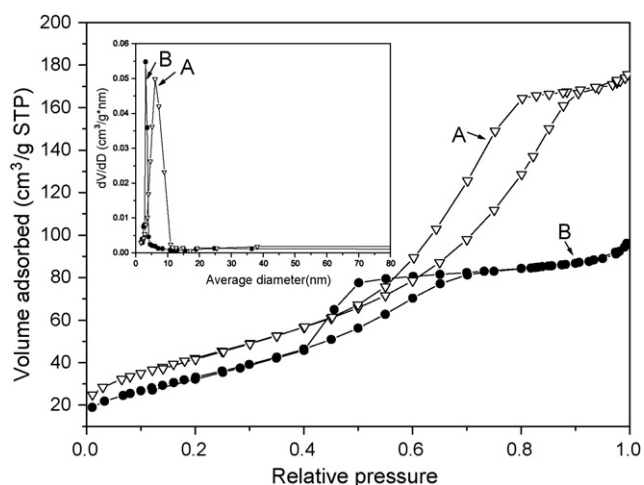


Fig. 6. N₂ adsorption/desorption isotherms of mesoporous TiO_{2-x}N_x samples: (A) MU-TiO_{2-x}N_x calcined at 350 °C; (B) M-TiO_{2-x}N_x calcined at 350 °C.

condensation of the mesoporous pore channels. The BET surface area, pore size, and pore volume of the samples are summarized in Table 1. The BET surface area of the mesoporous TiO_{2-x}N_x prepared with ultrasonic treatment (180.2 m²/g) is much larger than that without sonication (122.7 m²/g). Meanwhile, the average pore size and the pore volume are increased from 3.4 nm to 6.7 nm and

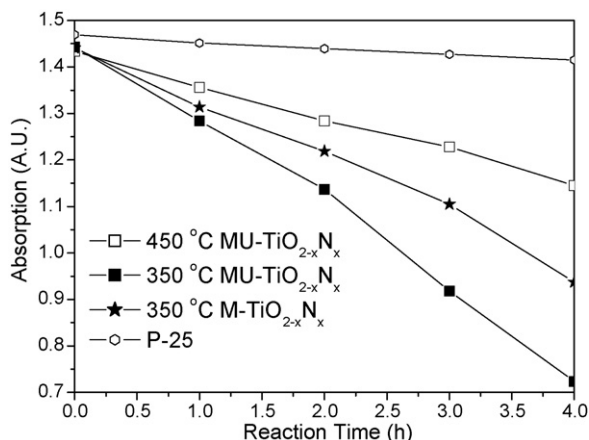
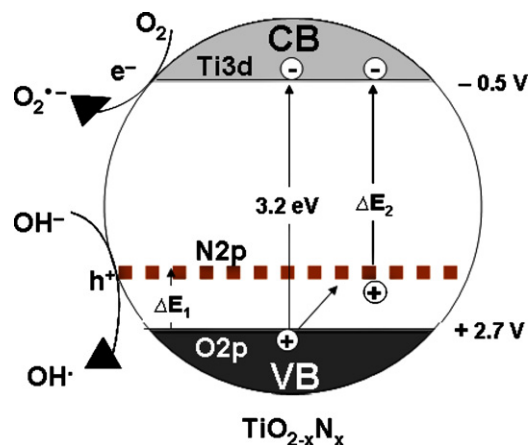


Fig. 7. Comparison of the photoactivity of different samples.



Scheme 2. Mechanism of TiO_{2-x}N_x visible-light photocatalysis.

0.14 cm³/g to 0.27 cm³/g, respectively. Such mesoporous architecture with large surface area and pore volume plays an important role in catalyst design for improving the adsorption of reactant molecules [27–30].

3.5. Photocatalytic oxidation of methylene blue

The decomposition of methylene blue was used to evaluate the photocatalytic performance of the mesoporous TiO_{2-x}N_x samples. Fig. 7 shows that all mesoporous TiO_{2-x}N_x samples show very high decomposition percentage attributed to the effect of nitrogen doping into the TiO₂ lattice. The photocatalytic performance of the mesoporous samples is further enhanced by the ultrasound pretreatment process. This is because ultrasound irradiation can increase the doped nitrogen content and enlarge the surface area of the photocatalysts. The optimum calcination temperature is 350 °C. Samples calcined at elevated temperatures show lower activity due to the loss of the nitrogen dopant.

As shown in Scheme 2, the occupied midgap (N-2p) level is slightly above the top of the (O-2p) valence band. Visible-light illumination produces “holes” in the midgap level, whereas UV irradiation produces holes in the (O-2p) valence band [31]. Doping nitrogen atoms into TiO₂ lattice effectively decreases the anatase band gap from 3.2 eV to 2.2 eV. This makes the utilization of visible-light feasible in photoreactions. Charge separation occurs upon

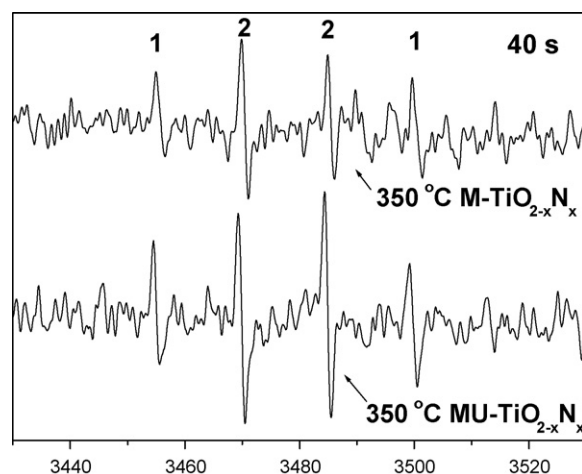


Fig. 8. ESR signals of the DMPO-OH• adducts in the mesoporous TiO_{2-x}N_x-DMPO dispersion. The signals were recorded after illumination for 40 s with a Quanta-Ray Nd:YAG pulsed laser operated in the continuous mode at 10 Hz frequency.

illumination. The adsorbed O_2 on the surface of the photocatalyst traps an electron excited from the valence band of $TiO_{2-x}N_x$ to form a superoxide anion radical ($O_2^{\bullet-}$). Meanwhile, the hole in the valence band is captured by the surface-bound OH^- to form a hydroxyl radical (OH^\bullet) [1].

Fig. 8 shows the EPR spectra for the DMPO- OH^\bullet spin adducts generated on visible-light illuminated mesoporous $TiO_{2-x}N_x$ samples. The characteristic 1:2:2:1 quadruple peaks confirm the formation of reactive oxygen species such as hydroxyl radicals [32]. The intensity of the peaks for MU- $TiO_{2-x}N_x$ is obviously stronger than that for M- $TiO_{2-x}N_x$. The MU- $TiO_{2-x}N_x$ sample is photocatalytically more active than the M- $TiO_{2-x}N_x$ sample because more OH^\bullet radicals are produced on its surface.

4. Conclusions

Mesoporous $TiO_{2-x}N_x$ nanohybrids were synthesized through in situ pyrolysis of the product from a chelation reaction between $TiCl_4$ and ethylenediamine in an ethanol solution of F127. A simple ultrasound pretreatment process could effectively enhance the activity of the photocatalyst by providing a higher nitrogen dopant concentration and a larger surface area.

Acknowledgement

This work was partially supported by the Innovation and Technology Fund of the Hong Kong Special Administrative Region, China.

References

- [1] M.R. Hoffmann, S.T. Martin, W. Choi, D.W. Bahnemann, Environmental applications of semiconductor photocatalysis, *Chem. Rev.* 95 (1995) 69–96.
- [2] Y. Kuroda, T. Mori, K. Yagi, N. Makihata, Y. Kawahara, M. Nagao, S. Kittaka, Preparation of visible-light-responsive $TiO_{2-x}N_x$ photocatalyst by a sol-gel method: analysis of the active center on TiO_2 that reacts with NH_3 , *Langmuir* 21 (2005) 8026–8034.
- [3] E. Borgarello, J. Kiwi, M. Graetzel, E. Pelizzetti, M. Visca, Visible light induced water cleavage in colloidal solutions of chromium-doped titanium dioxide particles, *J. Am. Chem. Soc.* 104 (1982) 2996–3002.
- [4] H. Kisch, L. Zang, C. Lange, W.F. Maier, C. Antonius, D. Meissner, Modified, amorphous titania—a hybrid semiconductor for detoxification and current generation by visible light, *Angew. Chem. Int. Ed.* 37 (1998) 3034–3036.
- [5] I. Nakamura, S. Sugihara, K. Takeuchi, Mechanism for NO photooxidation over the oxygen-deficient TiO_2 powder under visible light irradiation, *Chem. Lett.* 11 (2000) 1276–1277.
- [6] K. Takeuchi, I. Nakamura, O. Matsumoto, S. Sugihara, M. Ando, T. Ihara, Preparation of visible-light-responsive titanium oxide photocatalysts by plasma treatment, *Chem. Lett.* 12 (2000) 1354–1355.
- [7] J.C. Yu, J.G. Yu, W.K. Ho, Z.T. Jiang, L.Z. Zhang, Effects of F-doping on the photocatalytic activity and microstructures of nanocrystalline TiO_2 powders, *Chem. Mater.* 14 (2002) 3808–3816.
- [8] W.K. Ho, J.C. Yu, S.C. Lee, Synthesis of hierarchical nanoporous F-doped TiO_2 spheres with visible light photocatalytic activity, *Chem. Commun.* (2006) 1115–1117.
- [9] R. Asahi, T. Morikawa, T. Ohwaki, K. Aoki, Y. Taga, Visible-light photocatalysis in nitrogen-doped titanium oxides, *Science* 293 (2001) 269–271.
- [10] S.K. Joung, T. Amemiya, M. Murabayashi, K. Itoh, Mechanistic studies of the photocatalytic oxidation of trichloroethylene with visible-light-driven N-doped TiO_2 photocatalysts, *Chem. Eur. J.* 12 (2006) 5526.
- [11] H.M. Luo, C. Wang, Y.S. Yan, Synthesis of mesostructured titania with controlled crystalline framework, *Chem. Mater.* 15 (2003) 3841–3846.
- [12] X.C. Wang, J.C. Yu, H.Y. Yip, L. Wu, P.K. Wong, S.Y. Lai, A mesoporous Pt/ TiO_2 nanoarchitecture with catalytic and photocatalytic functions, *Chem. Eur. J.* 11 (2005) 2997–3004.
- [13] X.C. Wang, J.C. Yu, Y.L. Chen, L. Wu, X.Z. Fu, ZrO_2 -modified mesoporous nanocrystalline $TiO_{2-x}N_x$ as efficient visible light photocatalysts, *Environ. Sci. Technol.* 40 (2006) 2369–2374.
- [14] K.S. Suslick, *Sonochemistry*, *Science* 247 (1990) 1439–1445.
- [15] K.S. Suslick, S.B. Choe, A.A. Cichowlas, M.W. Grinstaff, Sonochemical synthesis of amorphous iron, *Nature* 353 (1991) 414–416.
- [16] W.P. Huang, X.H. Tang, Y.Q. Wang, Y. Koltypin, A. Gedanken, Selective synthesis of anatase and rutile via ultrasound irradiation, *Chem. Commun.* (2000) 1415–1416.
- [17] X.H. Tang, S.W. Liu, Y.Q. Wang, W.P. Huang, E. Sominski, O. Palchik, Y. Koltypin, A. Gedanken, Rapid synthesis of high quality MCM-41 silica with ultrasound radiation, *Chem. Commun.* (2000) 2119–2120.
- [18] G.S. Attard, J.C. Glyde, C.G. Goltner, Liquid-crystalline phases as templates for the synthesis of mesoporous silica, *Nature* 378 (1995) 366–368.
- [19] W.K. Ho, J.C. Yu, J. Lin, J.G. Yu, P.S. Li, Preparation and photocatalytic behavior of MoS_2 and WS_2 nanocluster sensitized TiO_2 , *Langmuir* 20 (2004) 5865–5869.
- [20] J.C. Yu, G.S. Li, X.C. Wang, X.L. Hu, C.W. Leung, Z.D. Zhang, An ordered cubic Im3m mesoporous Cr- TiO_2 visible light photocatalyst, *Chem. Commun.* (2006) 2717–2719.
- [21] T.L. Ma, M. Akiyama, E. Abe, I. Imai, High-efficiency dye-sensitized solar cell based on a nitrogen-doped nanostructured titania electrode, *Nano Lett.* 5 (2005) 2543–2547.
- [22] X.B. Chen, Y.B. Lou, A. Samia, C. Burda, J.L. Gole, Formation of oxynitride as the photocatalytic enhancing site in nitrogen-doped titania nanocatalysts: comparison to a commercial nanopowder, *Adv. Funct. Mater.* 15 (2005) 41–49.
- [23] H.X. Li, J.X. Li, Y.N. Huo, Highly active $TiO_{2-x}N_x$ photocatalysts prepared by treating TiO_2 precursors in NH_3 /ethanol fluid under supercritical conditions, *J. Phys. Chem. B* 110 (2006) 1559–1565.
- [24] R.L. Putnam, N. Nakagawa, K.M. McGrath, N. Yao, I.A. Aksay, S.M. Gruner, A. Navrotsky, Titanium dioxide-surfactant mesophases and Ti-TMS1, *Chem. Mater.* 9 (1997) 2690–2693.
- [25] I. Justicia, P. Ordejon, G. Canto, J.L. Mozos, J. Fraxedas, G.A. Battiston, R. Gerbasi, A. Figueras, Designed self-doped titanium oxide thin films for efficient visible-light photocatalysis, *Adv. Mater.* 14 (2002) 1399–1402.
- [26] H.X. Li, G.S. Li, J. Zhu, Y. Wan, Preparation of an active SO_4^{2-}/TiO_2 photocatalyst for phenol degradation under supercritical conditions, *J. Mol. Catal. A: Chem.* 226 (2005) 93–100.
- [27] D.R. Rolison, Catalytic nanoarchitectures—the importance of nothing and the unimportance of periodicity, *Science* 299 (2003) 1698–1701.
- [28] A.T. Bell, The impact of nanoscience on heterogeneous catalysis, *Science* 299 (2003) 1688–1691.
- [29] X.C. Wang, J.C. Yu, C.M. Ho, A.C. Mak, A robust three-dimensional mesoporous Ag/ TiO_2 nanohybrid film, *Chem. Commun.* (2005) 2262–2264.
- [30] G.S. Li, J.C. Yu, J. Zhu, Y. Cao, Hierarchical mesoporous grape-like titania with superior recyclability and photoactivity, *Micro. Meso. Mater.* 106 (2007) 278–283.
- [31] R. Nakamura, T. Tanaka, Y. Nakato, Mechanism for visible light responses in anodic photocurrents at N-doped TiO_2 film electrodes, *J. Phys. Chem. B* 108 (2004) 10617–10620.
- [32] S. Horikoshi, H. Hidaka, N. Serpone, Hydroxyl radicals in microwave photocatalysis. Enhanced formation of OH radicals probed by ESR techniques in microwave-assisted photocatalysis in aqueous TiO_2 dispersions, *Chem. Phys. Lett.* 376 (2003) 475–480.